Physiological Modeling of Altered Pharmacokinetics of a Novel Anticancer Drug, UCN-01 (7-Hydroxystaurosporine), Caused by Slow Dissociation of UCN-01 from Human α_1-Acid Glycoprotein

Eiichi Fuse,[1] Akitoshi Hashimoto,[1] Natsuko Sato,[1] Hiromi Tanii,[1] Takashi Kuwabara,[1,3] Satoshi Kobayashi,[1] and Yuichi Sugiyama[2]

Received January 18, 1999; accepted February 15, 2000

Purpose. The extremely low clearance and small distribution volume of UCN-01 in humans could be partly due to the high degree of binding to hAGP (1,2). The quantitative effects of hAGP on the pharmacokinetics of UCN-01 at several levels of hAGP and UCN-01 were estimated in rats given an infusion of hAGP to mimic the clinical situation and a physiological model for analysis was developed.

Methods. The plasma concentrations of UCN-01 (72.5–7250 nmol/kg iv) in rats given an infusion of hAGP, 15 or 150 nmol/h/kg, were measured by HPLC. Pharmacokinetic analysis under conditions assuming rapid equilibrium of protein binding and incorporating the dissociation rate was conducted.

Results. The Vdss and CLtot of UCN-01 (725 nmol/kg iv) in rats given an infusion of hAGP, 150 nmol/h/kg, fell to about 1/250 and 1/700 that in control rats. The Vdss and CLtot following 72.5–7250 nmol/kg UCN-01 to rats given 150 nmol/h/kg hAGP were 63.9–688 ml/kg and 3.18–32.9 ml/h/kg, respectively, indicating non-linearity due to saturation of UCN-01 binding. The CLtot estimated by the physiological model assuming rapid equilibrium of UCN-01 binding to hAGP, was six times higher than the observed value while the CLtot estimated by the model incorporating k_{off}, measured using DCC, was comparable with the observed value.

Conclusions. These results suggest that the slow dissociation of UCN-01 from hAGP limits its disposition and elimination.

KEY WORDS: α_1-acid glycoprotein; protein binding; dissociation rate; species difference; physiological model; pharmacokinetics.

INTRODUCTION

UCN-01 (7-hydroxystaurosporine) is a selective inhibitor of PKC, a key enzyme involved in signal transduction (3). It inhibits the growth of various cultured human and murine solid tumor cells *in vitro* and *in vivo* (4–6). Also, induction of G_1-phase accumulation by the drug, which might be mediated via inhibition of CDK2, has been reported (7,8). In addition, UCN-01 synergistically enhances the antitumor activity of several standard agents in cultured cancer cells *in vitro* and *in vivo* (9–11).

Phase I studies of UCN-01 have started in the United States and Japan which will investigate its role as a novel anticancer drug regulating the cell cycle. The plasma concentrations of UCN-01 in Phase I studies were much higher than expected from non-clinical data (1,12). The pharmacokinetic properties of UCN-01 in cancer patients were very different from those seen in dogs, rats and mice, and were characterized by low clearance with a small distribution volume (1,12). The CLtot, Vdss and $t_{1/2}$ in these animals were 600–4000 ml/h/kg, 6000–17000 ml/kg and 3–12 h, respectively (1,12). On the other hand, the CLtot, Vdss and $t_{1/2}$ after iv infusion to cancer patients were 0.04–0.25 ml/h/kg, 80–160 ml/kg, and 250–1700 h (1), respectively.

Previous studies (1,2) suggest that this dramatic species-difference in the pharmacokinetics of UCN-01 could, at least in part, be explained by high affinity binding to hAGP. There are several reasons for this. 1) There is a substantial species-difference in UCN-01 binding to AGP. The Ka of UCN-01 for hAGP is 8×10^8 $(M)^{-1}$, indicating very high affinity. On the other hand, the Ka for dog AGP was 1/60 that for hAGP. In rats, only nonspecific binding with a low affinity of UCN-01 for AGP was found. 2) Bound UCN-01, which is not removed by treatment with dextran-coated charcoal (DCC), is found in particular high concentrations in solutions of hAGP and human plasma. 3) Simultaneous iv administration of UCN-01 with hAGP apparently reduces the Vdss, CLtot and hepatic extraction of UCN-01 in rats. 4) Uptake of UCN-01 by isolated rat hepatocytes is also inhibited by adding hAGP to the medium.

In our previous study (2), the plasma levels of hAGP

[1] Drug Development Research Laboratories, Pharmaceutical Research Institute, Kyowa Hakko Kogyo Co., Ltd., 1188, Shimotogari, Nagaizumi-Cho, Sunto-Gun, Shizuoka 411-8731, Japan.

[2] Graduate School of Pharmaceutical Sciences, The University of Tokyo, 7-3-1, Hongo, Bunkyo-Ku, Tokyo 113-0033, Japan.

[3] To whom correspondence should be addressed. (e-mail; takashi.kuwabara@kyowa.co.jp)

ABBREVIATIONS: UCN-01, 7-hydroxystaurosporine; PKC, Ca^{2+}- and phospholipid-dependent protein kinase; CDK2, cyclin-dependent kinase 2; hAGP, human α_1-acid glycoprotein; AGP, α_1-acid glycoprotein; DCC, dextran-coated charcoal; k_{off}, dissociation rate constant; k_{on}, association rate constant; Kd ($=k_{off}/k_{on}$), equilibrium dissociation constant; Ka ($=k_{on}/k_{off}$), equilibrium association constant; f_p, unbound fraction in plasma; CLtot, systemic clearance; Vdss, apparent distribution volume at steady-state; $t_{1/2}$, elimination half-life; MRT, mean residence time; $AUC_{0-\infty}$, area under the plasma concentration-time curve; AUMC, area under the moment curve; $C_{b,v}$, and $C_{u,v}$, bound and unbound plasma concentrations of UCN-01 in the hepatic vein, $C_{b,a}$, and $C_{u,a}$, bound and unbound plasma concentrations of UCN-01 in the systemic artery; k'_{on}, and k'_{off}, association rate constant and dissociation rate constant of UCN-01 for binding-protein; k_{on}, and k_{off}, association rate constant and dissociation rate constant of UCN-01 for hAGP; P'_u, unbound concentration of binding-protein (i.e., total binding-protein concentration − bound UCN-01 concentration); n', number of UCN-01 binding sites per molecule of binding-protein; P_u, unbound concentration of hAGP; n, number of UCN-01 binding sites per molecule of hAGP; $n'P'_u$, binding capacity of UCN-01 with binding-protein; nP_u, binding capacity of UCN-01 with hAGP; CLint, intrinsic clearance of UCN-01 in liver; Q, blood flow rate in liver; R, R_b, and R_u, ratio of total, bound and unbound concentration of UCN-01 in blood to that in plasma; V_E, and V_H, extracellular and total volume in liver; V_b, V_u, distribution volume for bound and unbound drug in the blood pool; K_p, ratio of total concentration of UCN-01 in liver and hepatic venous plasma, $K_{p,u}$, ratio of total concentration of UCN-01 in liver to unbound plasma concentration of UCN-01 in the hepatic vein; $C_{t,0}$, $C_{b,0}$, $C_{u,0}$, total, bound and unbound concentrations of UCN-01 in plasma at time zero; V_1, apparent distribution volume of the plasma compartment; f_R, unbound fraction of UCN-01 in erythrocytes; Pss, concentration of hAGP at steady state.

after simultaneous bolus administration of UCN-01 gradually declined with a half-life of ca. 17 h. Although hAGP is an acute phase protein and intra-patient variation due to certain diseases such as cancer is known, the levels are generally maintained at 10–25 μM under normal physiological conditions (13). UCN-01 and hAGP were administered only at one dose in the previous study. In this paper, the effect of hAGP on the pharmacokinetics of UCN-01 at three different doses of UCN-01 has been estimated in rats at two infusion rates of hAGP to mimic the situation in humans. In addition, the high concentration of UCN-01 remaining 0.1 and 2 h after adding DCC to a solution of hAGP implies that the dissociation half-life of UCN-01 from hAGP is much slower than from the plasma proteins of experimental animals and other human plasma proteins. The dissociation half-life from hAGP was estimated to be ca. 2 h and much longer than that of other ligands from plasma proteins, generally only a few milliseconds (14). In general, only unbound drug can cross biological membrane and play a role in determining its distribution and elimination. Therefore, the slow dissociation of UCN-01 may alter its pharmacokinetics in humans. In addition, in contrast to humans, the CLtot in rats is extremely high (ca. 3000 ml/h/kg) and depends on organ blood flow (12). The CLtot was reduced markedly by the high degree of binding of UCN-01 to hAGP in the rats given hAGP and was not limited by blood flow (2). For a kinetic analysis of both conditions, with and without hAGP using an identical model, organ blood flow should be incorporated in the model. In addition, the dissociation of UCN-01 from hAGP seems to be slow (2) and the dissociation/association of UCN-01 and hAGP as well as the general process of protein binding, i.e., rapid equilibrium conditions, should be considered in the model. Accordingly, in this paper, we have quantitatively measured the *in vitro* k_{off} of UCN-01 from hAGP and developed a physiological model incorporating the k_{off} and k_{on} for UCN-01 pharmacokinetics in rats given hAGP by infusion. For comparison, a kinetic analysis was also performed assuming rapid equilibrium in protein binding.

MATERIALS AND METHODS

Chemicals and Reagents

UCN-01 and staurosporine, as the internal standard (I.S.) for HPLC analysis, were produced as described previously (3). hAGP was purchased from Saikin Kagaku Institute (Sendai, Japan). DCC, to which proteins exhibited little non-specific binding, was prepared by the method reported previously (2). DCC was added to an equal volume of human plasma or hAGP solution (20 μM) and the final DCC concentrations were 40, 20 and 10 mg charcoal/ml. Distilled water was purified by Milli Q Labo (Nihon Millipore, Tokyo). All other chemicals and solvents were of analytical grade.

Human Plasma and Animals

Blood collected from a healthy volunteer, following written informed consent, was centrifuged to provide control plasma for measuring the *in vitro* dissociation rate. Male SD strain rats, 6 to 8 weeks of age (Nihon SLC, Hamamatsu, Japan, 270 to 300 g at the start of the experiments), were housed for about one week under controlled conditions with free access to food and water except during the cannulation procedure and 8 h after the start of dosing. The experiments were approved by the Welfare Committee for Experimental Animals in our institute.

Preparation of Dosing Solution

UCN-01

The dosing solution of UCN-01 was prepared by the previous method (12). All dosing solutions were kept on ice and protected from light until administered to rats.

hAGP

hAGP was dissolved in physiological saline for injection just before the start of dosing. The concentrations of hAGP for a loading dose were 9.81 or 0.981 mg/ml and the doses were 19.6 or 1.96 mg/kg (467 or 46.7 nmol/kg, molecular weight; 42000). The dosing solutions for infusion prepared at concentrations of 2.1 or 0.21 mg/ml were diluted with saline according to the body weight of the rats. The dosing rates were 6.3 or 0.63 mg/h/kg (150 or 15 nmol/h/kg). As a control, equal volumes of saline without hAGP were administered to rats.

Animal Experiment

Rats were anesthetized with diethylether and cannulated with polyethylene tubing (PE50, Becton Dickinson and Company, Parsippany, NJ, USA) into the jugular vein. The rats were kept in restrainers (KN-325 (A), Natsume Seisakusyo, Tokyo, Japan) and, after recovery from the anesthesia, hAGP was infused via the cannula using a micro automatic syringe pump (CFV-3100, Nihon Kohden, Tokyo, Japan). The infusion rate was set at 0.9 ml/h/rat. The infusion was started immediately after bolus administration of hAGP as a loading dose, at a volume of 2 ml/kg. Bolus administration of UCN-01 to rats was carried via the same venous cannula connected to a three-way stopcock, at a volume of 2 ml/kg, 1 h after the start of the hAGP infusion. Immediately after bolus dosing of hAGP or UCN-01, the remainder of the dosing solution in the cannula was administered using the infusion solution. To analyze the plasma concentrations of UCN-01 and hAGP, ca. 0.25 ml blood was withdrawn from the tail vein and transferred to heparinized capillary tubes at designed times. Each plasma sample was separated by centrifugation and stored at −70°C until assayed.

Determination of Dissociation Rate

UCN-01 dissolved in dimethyl sulfoxide was diluted with hAGP or plasma. DCC was added to an equal volume of hAGP solution or plasma to give a final concentration of 5 μM UCN-01 at 37°C. Then, the suspension was agitated for a few seconds. Immediately (time zero), 0.1, 0.25, 0.5, 1, 2 and 4 h after mixing, an aliquot was centrifuged at 4°C, ca. 20000x g, for 3 min and the supernatant was used to measure the UCN-01 concentration. The remaining percentage was calculated from the relative I.S. ratio of the peak height at each point to that at time 0. The slope of the plot of the logarithm of the remaining percentage versus time gave the apparent dissociation rate constant (k_{off}).

Determination of UCN-01 and hAGP Concentrations

The UCN-01 and hAGP concentrations were determined by HPLC and ELISA as reported previously (2,15). The range for quantitation was 0.2–100 ng/ml for UCN-01 and 100–2500 ng/ml for hAGP. The accuracy and precision of the intra- and inter-day assays were within ±15% for UCN-01 and ±20% for hAGP. There was no cross-reactivity with rat AGP and UCN-01 had no effect on the ELISA method.

Pharmacokinetic Analysis

The time-course of total UCN-01 concentrations in plasma was analyzed in individual rats using a model-independent approach with the linear least square method (16,17). The slope of the elimination phase (elimination rate constant: k) in the plot of the logarithm of the plasma concentration versus time was determined by log-linear regression analysis of the last three points (4, 8 and 24 h). The $t_{1/2}$ was calculated as 0.693/k. The $C_{t,0}$ was extrapolated by log-linear regression analysis of the first three points (0.1, 0.25 and 1 h). The $AUC_{0-\infty}$ and AUMC were determined by the trapezoidal rule using $C_{t,0}$ and the observed data with extrapolation to infinity using k. The CLtot, MRT and Vdss were calculated as $Dose/AUC_{0-\infty}$, AUMC/AUC and CLtot × MRT.

Statistical Analysis

All data are presented as the mean ± S.D. of three animals or experiments. The value "0" was used when the UCN-01 concentration in one of the three rats was below the lower limit of quantitation (0.2 ng/ml). Statistical analysis was carried out using Windows-SAS System Release 6.12 (SAS Institute, Cary, NC, USA). The effects of hAGP or UCN-01 doses on the pharmacokinetic parameters of UCN-01 were estimated by Dunnett's or Tukey's test after identifying equal variance and any significant difference by Bartlett's test and a one-way analysis of variance, respectively. In the case of a significant difference in variance, the analysis was discontinued. Any significant difference in the k_{off} of UCN-01 among the concentrations of DCC or the other materials (hAGP and plasma) was estimated by a one-way analysis of variance followed by Tukey's test. For all tests, a probability of $p < 0.05$ was considered statistically significant.

Model Development

The mass-balance rate equations for the blood pool and liver on the basis of bound and unbound concentrations in plasma for control rats in Fig. 1 can be written as shown below:

$$V_E \cdot dC_{b,v}/dt = k'_{on} \cdot n'P'_u \cdot V_E \cdot C_{u,v} - k'_{off} \cdot C_{b,v} \cdot V_E + Q \cdot R_b \cdot (C_{b,a} - C_{b,v}) \quad (1)$$

$$K_{p,u} \cdot V_H \cdot dC_{u,v}/dt = k'_{off} \cdot C_{b,v} \cdot V_E - k'_{on} \cdot n'P'_u \cdot V_E \cdot C_{u,v} - CLint \cdot C_{u,v} + Q \cdot R_u \cdot (C_{u,a} - C_{u,v}) \quad (2)$$

$$V_b \cdot dC_{b,a}/dt = k'_{on} \cdot n'P'_u \cdot V_b \cdot C_{u,a} - k'_{off} \cdot C_{b,a} \cdot V_b + Q \cdot R_b \cdot (C_{b,v} - C_{b,a}) \quad (3)$$

$$V_u \cdot dC_{u,a}/dt = k'_{off} \cdot C_{b,a} \cdot V_b - k'_{on} \cdot n'P'_u \cdot V_b \cdot C_{u,a} + Q \cdot R_u \cdot (C_{u,v} - C_{u,a}) \quad (4)$$

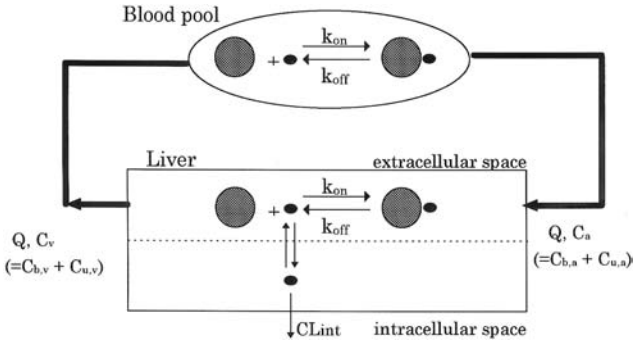

Fig. 1. Physiological and pharmacokinetic models for the elimination of UCN-01. CLint; intrinsic clearance of UCN-01 in liver. Q; blood flow rate in liver, k_{off}; dissociation rate constant of UCN-01, k_{on}; association rate constant of UCN-01, $C_{b,a}$; bound plasma concentrations of UCN-01 in the systemic artery, $C_{u,a}$; unbound plasma concentrations of UCN-01 in the systemic artery, $C_{b,v}$; bound plasma concentrations of UCN-01 in the hepatic vein, $C_{u,v}$; unbound plasma concentrations of UCN-01 in the hepatic vein, C_a; total plasma concentrations of UCN-01 in the systemic artery, C_v; total plasma concentrations of UCN-01 in the hepatic vein.

while those for rats given hAGP infusions are:

$$V_E \cdot dC_{b,v}/dt = k'_{on} \cdot n'P'_u \cdot V_E \cdot C_{u,v} - k'_{off} \cdot C_{b,v} \cdot V_E + k_{on} \cdot nP_u \cdot V_E \cdot C_{u,v} - k_{off} \cdot C_{b,v} \cdot V_E + Q \cdot R_b \cdot (C_{b,a} - C_{b,v}) \quad (1')$$

$$K_{p,u} \cdot V_H \cdot dC_{u,v}/dt = k'_{off} \cdot C_{b,v} \cdot V_E - k'_{on} \cdot n'P'_u \cdot V_E \cdot C_{u,v} + k_{off} \cdot C_{b,v} \cdot V_E - k_{on} \cdot nP_u \cdot V_E \cdot C_{u,v} - CLint \cdot C_{u,v} + Q \cdot R_u \cdot (C_{u,a} - C_{u,v}) \quad (2')$$

$$V_b \cdot dC_{b,a}/dt = k'_{on} \cdot n'P'_u \cdot V_b \cdot C_{u,a} - k'_{off} \cdot C_{b,a} \cdot V_b + k_{on} \cdot nP_u \cdot V_b \cdot C_{u,a} - k_{off} \cdot C_{b,a} \cdot V_b + Q \cdot R_b \cdot (C_{b,v} - C_{b,a}) \quad (3')$$

$$V_u \cdot dC_{u,a}/dt = k'_{off} \cdot C_{b,a} \cdot V_b - k'_{on} \cdot n'P'_u \cdot V_b \cdot C_{u,a} + k_{off} \cdot C_{b,a} \cdot V_b - k_{on} \cdot nP_u \cdot V_b \cdot C_{u,a} + Q \cdot R_u \cdot (C_{u,v} - C_{u,a}) \quad (4')$$

The binding-protein represents the main binding protein in control rats and it has not been identified yet. In this study, the plasma concentrations of UCN-01 in control rats were less than 0.1 μM and were much lower than those of AGP or albumin. Accordingly, the protein binding was assumed to be linear. In the following analysis, the n′P′ in control rats was defined as 20 μM, i.e., a normal level of AGP. It was confirmed that the results were almost identical when n′P′ was set at 600 μM, i.e., a normal level of albumin (data not shown). In this model, the liver was assumed to be the only organ involved in the elimination of UCN-01 since the main clearance mechanism of UCN-01 is hepatic metabolism (12). And, assuming that only unbound UCN-01 can cross biological membranes and the rate of metabolism depends on the unbound UCN-01 surrounding the enzymatic site, the processes of membrane-permeability, distribution into tissues and metabolism, except for the interaction of UCN-01 with hAGP, reach equilibrium rapidly, i.e., the "well-stirred model" (18). The unbound and bound concentrations of UCN-01 in hepatic extracellular fluid are also assumed to be equal to those in hepatic venous plasma. Although

there is little evidence for the rapid equilibrium in the intracellular space, the assumption was made since the *in vitro* uptake of ^{3}H-UCN-01 into isolated rat hepatocytes (2) and the *in vivo* ratio of the ^{3}H-UCN-01 concentration in liver to that in plasma after administering ^{3}H-UCN-01 to rats (unpublished data) reached constant values relatively rapidly. In the case of rats given an infusion of hAGP, the amount of UCN-01 interacting with the binding-protein in control rats can be neglected since most of the UCN-01 in plasma binds to hAGP. Therefore, in the following analysis, (Eqs. 1′–4′) were transformed to (Eqs. 1a–4a) shown below.

$$V_E \cdot dC_{b,v}/dt = k_{on} \cdot nP_u \cdot V_E \cdot C_{u,v} - k_{off} \cdot C_{b,v} \cdot V_E + Q \cdot R_b \cdot (C_{b,a} - C_{b,v}) \quad (1a)$$

$$K_{p,u} \cdot V_H \cdot dC_{u,v}/dt = k_{off} \cdot C_{b,v} \cdot V_E - k_{on} \cdot nP_u \cdot V_E \cdot C_{u,v} - CLint \cdot C_{u,v} + Q \cdot R_u \cdot (C_{u,a} - C_{u,v}) \quad (2a)$$

$$V_b \cdot dC_{b,a}/dt = k_{on} \cdot nP_u \cdot V_b \cdot C_{u,a} - k_{off} \cdot C_{b,a} \cdot V_b + Q \cdot R_b \cdot (C_{b,v} - C_{b,a}) \quad (3a)$$

$$V_u \cdot dC_{u,a}/dt = k_{off} \cdot C_{b,a} \cdot V_b - k_{on} \cdot nP_u \cdot V_b \cdot C_{u,a} + Q \cdot R_u \cdot (C_{u,v} - C_{u,a}) \quad (4a)$$

The plasma concentration-time profiles of the administered hAGP did not change over the range of doses of UCN-01 tested (data not shown). The products of the concentrations of hAGP (11.9 μM or 1.10 μM) in the rats undergoing hAGP infusion described later and n (0.794) were used as the nP in this model. Both "n" and "Ka" were determined by analysis using the ultracentrifugation procedure reported previously (1) (data not shown).

Modeling Analysis of Protein Binding Under Linear Conditions

Under linear conditions for the protein binding of UCN-01 (UCN-01 concentrations in plasma $<<$ nP_u), P_u is given by the total hAGP concentration. By applying the infinite theorem, after converting the differential equations (Eqs. 1a–4a) to Laplace transforms, the AUC for $C_{b,a}$, $C_{u,a}$, $C_{b,v}$, or $C_{u,v}$ was calculated and the CLtot, obtained by dividing the UCN-01 dose by the sum of $AUC_{b,a}$ + $AUC_{u,a}$ was obtained from the equation below (Appendix A);

$$\begin{aligned} CLtot = {} & (k_{off} \cdot V_b \cdot k_{off} \cdot V_E \cdot CLint \cdot Q \cdot R_u \\ & + k_{off} \cdot V_b \cdot Q \cdot R_b \cdot CLint \cdot Q \cdot R_u \\ & + k_{off} \cdot V_E \cdot Q \cdot R_b \cdot CLint \cdot k_{on} \cdot nP_u \cdot V_b \\ & + k_{off} \cdot V_E \cdot Q \cdot R_b \cdot CLint \cdot Q \cdot R_u)/ \\ & \{[Q \cdot R_b \cdot Q \cdot R_u \cdot (k_{on} \cdot nP_u \cdot V_E + k_{on} \cdot nP_u \cdot V_b + k_{off} \cdot V_E \\ & + k_{off} \cdot V_b) + Q \cdot R_u \cdot k_{off} \cdot V_E \cdot (k_{on} \cdot nP_u \cdot V_b + k_{off} \cdot V_b) \\ & + Q \cdot R_b \cdot k_{on} \cdot nP_u \cdot V_E \cdot (k_{on} \cdot nP_u \cdot V_b + k_{off} \cdot V_b)] \\ & + CLint \cdot [k_{off} \cdot V_E \cdot (k_{on} \cdot nP_u \cdot V_b + k_{off} \cdot V_b) \\ & + Q \cdot R_b \cdot (k_{on} \cdot nP_u \cdot V_b + k_{off} \cdot V_b)] \\ & + CLint \cdot (k_{off} \cdot V_E \cdot Q \cdot R_u + Q \cdot R_b \cdot Q \cdot R_u) \cdot k_{on} \cdot nP_u/ \\ & (k_{on} \cdot nP_u + k_{off}) + CLint \cdot (k_{off} \cdot V_E \cdot Q \cdot R_b) \cdot k_{off}/ \\ & (k_{on} \cdot nP_u + k_{off})\} \end{aligned} \quad (5)$$

where the relationship between k_{off} and CLtot was simulated using the experimental data and the literature values in Table I as described later. The V_b and V_u were estimated from the following equation, assuming that the binding of UCN-01 to proteins in blood as well as the passage across membranes and distribution into tissues occur immediately after administering UCN-01;

$$Dose = C_{t,0} \cdot V_1 = C_{b,0} \cdot V_b + C_{u,0} \cdot V_u \quad (6)$$

$C_{b,0}$ and $C_{u,0}$ were determined using the *in vitro* unbound fraction (0.0175; Ref. 1) and $C_{t,0}$ after giving UCN-01 at a dose of 725 nmol/kg to control rats. The V_1 after administering UCN-01 at the lowest dose, 72.5 nmol/kg, to rats given an infusion of hAGP (53.0 ml/kg) was estimated as V_b. The V_u was calculated as 491000 ml/kg from the above parameters using Eq. 6. The unbound concentration in erythrocytes was assumed to be the same as that in plasma. The R_b for control rats was calculated as 1.98 using Eq. 7 below and the ratio of the blood-to-plasma concentration, R (1.96; Ref. 12) in normal rats.

$$R = R_b \cdot (1 - f_p) + R_u \cdot f_p \quad (7)$$

The R_b for rats given an infusion of hAGP under linear conditions of protein binding was estimated as 1 − Ht (Ht; hematocrit, 0.46; Ref. 19), since the distribution of UCN-01 into erythrocytes is inhibited by the high degree of binding of UCN-01 to hAGP in plasma. As described later, in the analysis involving non-linear protein binding conditions, R_b was estimated to be a variable parameter calculated by Eq. 8, taking into consideration the saturable binding of UCN-01 to hAGP (Appendix B);

$$R_b = [f_R \cdot (1 - f_p) + Ht \cdot (f_p - f_R)]/f_R/(1 - f_p) \quad (8)$$

where f_R was postulated to be constant, i.e., linear binding of UCN-01 to erythrocytes. Assuming that the CLtot of UCN-01 is the same as the hepatic clearance and the passage across biological membranes as well as distribution into and elimination from tissues rapidly reaches equilibrium, the CLint can be calculated from the following equation based on the "well stirred model (18)".

$$CLint = Q \cdot R \cdot CLtot/(Q \cdot R - CLtot)/f_p \quad (9)$$

The CLint was calculated as 370000 ml/h/kg using the parameters for control rats in Table 1 and Eq. 9. The value was also used in rats given an infusion of hAGP as well as control rats. The relationship between the CLtot and k_{off} was estimated by changing the k_{off}, with the k_{on} fixed as the Kd, and using the parameters in Table I.

Modeling Analysis of Protein Binding Under Non-Linear Conditions

Under non-linear conditions, in addition to the above linear protein binding conditions, the plasma concentration-time profiles of UCN-01 in control rats and rats given an infusion of hAGP were simulated using the numerical method of Runge-Kutta gill (20). The parameters in Table I and the $K_{p,u}$ were used for the simulation. The K_p was obtained by fitting the following equations by the non-linear least square method

Table I. Pharmacokinetic and Physiological Parameters for the Models of UCN-01 in Control Rats and Rats Given an Infusion of hAGP

	V_b (ml/kg)	V_u (ml/kg)	V_E (ml/kg)	V_H (ml/kg)	CLint (ml/h/kg)	Q (ml/h/kg)	Kd (μM)	nP (μM)	R_b	R_u	f_R
contol rats	53.0	491000	11.9	40.0	370000	3630	0.356	20	1.98	1	0.00567
rats infused with hAGP	53.0	491000	11.9	40.0	370000	3630	0.000645	9.45	0.54	1	0.00567

Note: These parameters were determined as shown in the text and were used in the simulation of the concentrations of UCN-01 under linear conditions of protein binding, (UCN-01 concentrations << hAGP concentrations, in Fig. 6 and Fig. 7).

(MULTI-RUNGE, Ref. 21), assuming a rapid equilibrium in protein binding, (Eqs. 10–12), to the actual time-course of the plasma concentrations after giving UCN-01 at 725 nmol/kg, to control rats. The $K_{p,u}$ was calculated by dividing the K_p by the *in vitro* f_p in control rat plasma (1).

$$K_p \cdot V_H \cdot dC_v/dt = Q \cdot R \cdot (C_a - C_v) - f_p \cdot CLint \cdot C_v \quad (10)$$

$$V_1 \cdot dC_a/dt = Q \cdot R \cdot (C_v - C_a) \quad (11)$$

$$f_p = \{(C_t - nP - k_{off}/k_{on}) + [(Ct - nP - k_{off}/k_{on})^2 + 4 \cdot k_{off} \cdot C_t/k_{on}]^{0.5}\}/2/C_t \quad (12)$$

In (Eqs. 1–4) for control rats, the k_{off}/k_{on} was estimated from (Eq. 13) assuming that the protein binding in control rats was linear at the concentration where the *in vitro* f_p was measured.

$$f_p = (k_{off}/k_{on})/[(k_{off}/k_{on}) + nP] \quad (13)$$

The $C_{b,o}$ and $C_{u,o}$ in the simulation of UCN-01 concentrations after bolus iv administration of UCN-01 at 72.5 nmol/kg to rats given an infusion of hAGP (hAGP level; 11.9 μM) were calculated as Dose/V_b and 0, assuming that most of the UCN-01 in blood was rapidly bound to hAGP and the unbound UCN-01 could be neglected since the Dose/V_b was lower than the nP. In the simulation at UCN-01 doses of 725 and 7250 nmol/kg in the rats given an infusion of hAGP, the nP was estimated as the $C_{b,o}$ and the $C_{u,o}$ was calculated using the equation shown below.

$$C_{u,o} = (Dose - C_{b,o} \cdot V_b)/V_u \quad (14)$$

In the simulation of UCN-01 concentrations after administering UCN-01 at a dose of 725 nmol/kg to rats given an infusion at a rate of 15 nmol/h/kg, the $C_{b,o}$ was also estimated to be nP and the $C_{u,o}$ was determined using Eq. 14. Alternatively, a simulation assuming the rapid dissociation of UCN-01 from hAGP in rats given an infusion of hAGP was performed, where the k_{off} was set at 20000 h^{-1}, taking into consideration the relationship between k_{off} and CLtot (Fig. 6).

RESULTS

Plasma Concentration-Time Profiles of UCN-01 After Bolus Intravenous Administration of UCN-01 to Rats Infused with hAGP

The time-courses of the plasma concentrations of hAGP after bolus iv administration of UCN-01 at doses of 72.5 to 7250 nmol/kg, 1 h after bolus administration of hAGP at a dose of 46.7 or 467 nmol/kg, followed immediately by the infusion of hAGP at a dosing rate of 15 or 150 nmol/h/kg to rats are shown in Fig. 2. The plasma concentrations of hAGP at 0.1 h, the first sampling point, were 1.10 and 11.9 μM, respectively, and exhibited only slight increases thereafter. No difference in hAGP levels was found after different doses of UCN-01 (data not shown). The concentrations of hAGP at the two infusion rates were almost proportional to the rates. Hereafter, 1.10 and 11.9 μM are taken as the Pss, considering the timing of UCN-01 administration.

The plasma concentration-time profiles of UCN-01, after bolus iv administration of UCN-01 at 725 nmol/kg to rats with Pss levels of hAGP maintained at 1.10 and 11.9 μM, increased with the dosing rate of hAGP and the concentrations of UCN-01 extrapolated to time 0 were 12.5- and 110-fold those in control rats (Table II, Fig. 3). Furthermore, the levels of UCN-01 after giving a dose of 725 nmol/kg to rats infused with hAGP were comparable with those of hAGP, i.e., 1.10 and 11.9 μM (Table II). The Vdss in rats given an infusion of hAGP at each Pss fell to 1/33 or 1/248 that of control rats and the CLtot was reduced to 1/68 or 1/717 (Table II). Although the $t_{1/2}$ and MRT in the rats given an infusion of hAGP at the high Pss

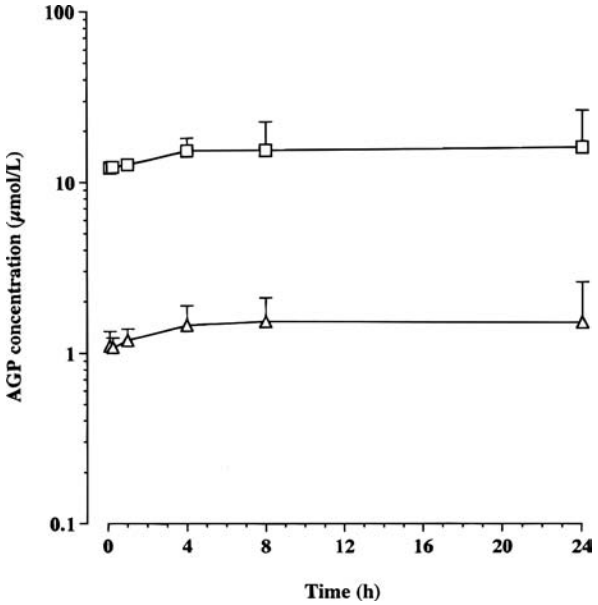

Fig. 2. Plasma concentration-time profiles of hAGP during iv infusion of hAGP to rats. The infusion of hAGP started immediately after iv administration of hAGP. The bolus dose of hAGP was 46.7 (△) or 467 (□) nmol/kg. The infusion rate of hAGP was 15 (△) or 150 (□) nmol/h/kg. UCN-01 was given as an iv bolus, at 725(△) or 72.5 (□) nmol/kg, 1 h after the start of infusion of hAGP. The horizontal axis represents the time after iv administration of UCN-01. Each value with a bar represents the mean + S.D. of 3 rats.

Table II. Model-Independent Pharmacokinetic Parameters of UCN-01 After Bolus IV Administration of UCN-01 to Rats Given an Infusion of hAGP

Dose		Plasma concentration		Pharmacokinetic parameter of UCN-01				
UCN-01 (μmol/kg)	hAGP (nmol/h/kg)	hAGP[a] (μM)	UCN-01[b] (μM)	t1/2 (h)	Vdss (ml/kg)	$AUCO_{0-\infty}$ (μg·h/ml)	CLtot (ml/h/kg)	MRT (h)
725	0	–	0.0839 ± 0.0116	6.95 ± 2.20	24200 ± 3900	0.105 ± 0.017	3390 ± 540	7.36 ± 2.37
725	150	12.7 ± 0.3	9.26 ± 1.00	15.3 ± 3.3	97.4 ± 7.1	75.5 ± 13.2	4.73 ± 0.82	21.2 ± 5.0
72.5	150	12.2 ± 0.7	1.39 ± 0.20	14.9 ± 2.5	63.9 ± 7.5	11.0 ± 0.6	3.18 ± 0.18	20.3 ± 3.5
7250	150	10.9 ± 0.2	12.8 ± 0.65	15.1 ± 1.7	688 ± 307	118 ± 40	32.9 ± 13.8	20.8 ± 2.3
725	15	1.10 ± 0.25	1.05 ± 0.03	11.4 ± 2.8	736 ± 90	7.46 ± 2.39	50.1 ± 14.8	15.5 ± 4.3

Note: Each value represents the mean ± S.D. of 3 animals. The pharmacokinetic parameters for the individual plasma concentration-time profiles of UCN-01 were calculated using model independent methods.
[a] hAGP concentration in plasma at steady-state.
[b] UCN-01 concentration in plasma extrapolated to time 0 using the log-linear regression of the data during 0.1–1 h.

were significantly longer than in controls ($p < 0.05$), they were only 1.6- to 2.9-fold greater than those in controls (Table II).

The ratios of the plasma concentration of UCN-01 extrapolated to time 0 after bolus iv administration of UCN-01 at 72.5, 725 or 7250 nmol/kg, i.e., dose ratios 1:10:100, to rats given an infusion of hAGP (Pss; 11.9 μM) were 1:6.7:9.2, indicating non-linear pharmacokinetics (Table II, Fig. 4). As shown in Table II, the Vdss increased with the dose and the ratios were 1:1.5:10 at each dose, respectively. The CLtot also increased in a similar way. The value at the highest dose, 7250 nmol/kg, was high. The $t_{1/2}$ and MRT in rats given an infusion of hAGP at 150 nmol/h/kg were independent of the dose of UCN-01.

Dissociation Rate of UCN-01 from hAGP or Human Plasma Proteins

The time-courses of UCN-01 remaining in the supernatants after adding DCC to hAGP, at 10, 20 and 40 mg/ml suspension at 37°C, are shown in Fig. 5. No significant difference in the slope, i.e., k_{off}, between DCC concentrations of 20 and 40 mg/ml was found and the values were 0.346 ± 0.016 and 0.383 ± 0.054 h^{-1}. The dissociation half-life calculated from the k_{off} was approximately 2 h. The k_{off} in human plasma was 0.150 ± 0.010 h^{-1} and was significantly lower than in hAGP solution ($p = 0.0087$, data not shown).

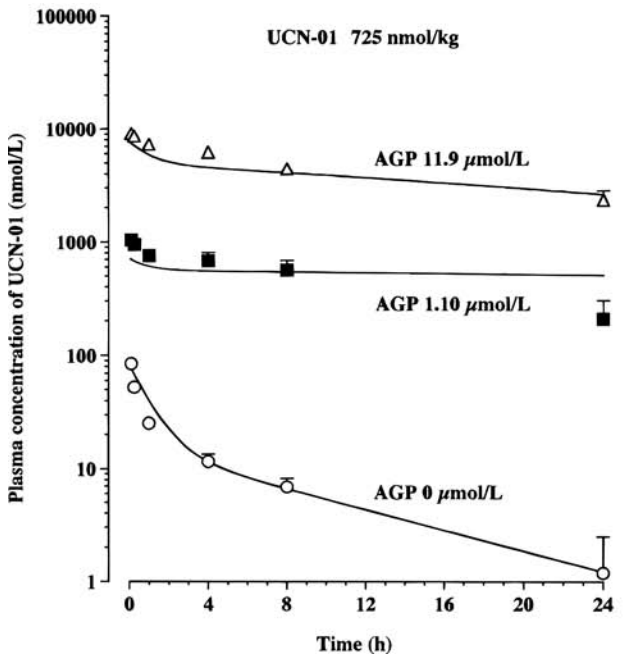

Fig. 3. Plasma concentration-time profiles of UCN-01 after iv administration of UCN-01 at a dose of 725 nmol/kg of UCN-01 to rats given an infusion of hAGP at dosing rates of 0 (○), 15 (■) and 150 (△) nmol/h/kg. Each value with a bar represents the mean + S.D. of 3 rats. Each line represents the data simulated from the model shown in Fig. 1.

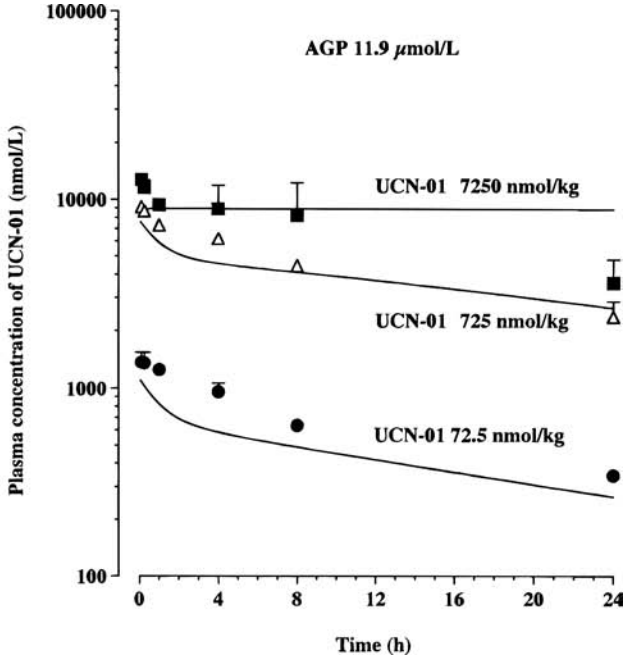

Fig. 4. Plasma concentration-time profiles of UCN-01 after iv administration of UCN-01, at doses of 72.5 (●), 725 (△) and 7250 (■) nmol/kg of UCN-01, to rats given an infusion of hAGP at a dosing rate of 150 nmol/h/kg. Each value with a bar represents the mean + S.D. of 3 rats. Each line represents the data simulated from the model shown in Fig. 1.

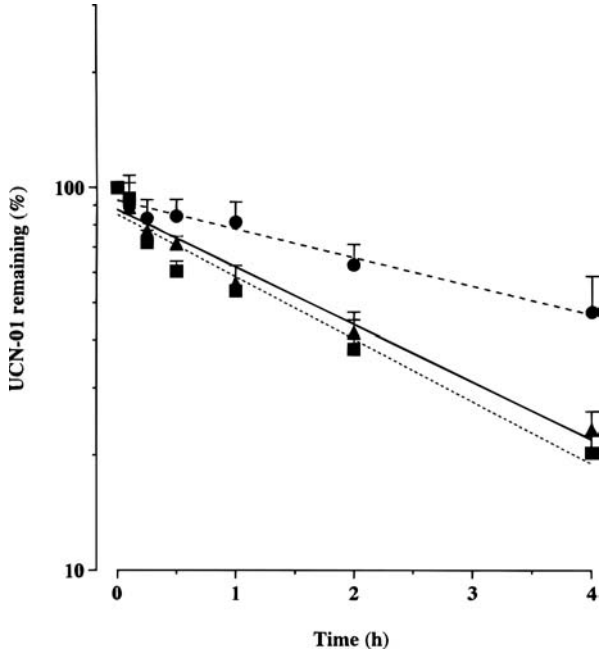

Fig. 5. Remaining ratio-time profiles of UCN-01 after adding dextran-coated charcoal to hAGP solution. Each symbol with a bar represents the mean + S.D. of 3 experiments. Final charcoal concentrations were 10 (●), 20 (▲), and 40 (■) mg/ml suspension. The dashed, solid and dotted lines are regression curves for (●); Remaining ratio = $92.7 \times e^{(-0.173 \times \text{Time})}$, r = 0.971, for (▲); = $87.7 \times e^{(-0.346 \times \text{Time})}$, r = 0.976, and for (■); = $85.0 \times e^{(-0.375 \times \text{Time})}$, r = 0.951.

Modeling Analysis

Relationship Between k_{off} and the Calculated CLtot

Each CLtot in rats given an infusion of hAGP and control rats corresponding to the range of the k_{off} of UCN-01 was calculated using equation 5 under conditions of linear pharmacokinetics, including protein binding (Fig. 6). The physiological and pharmacokinetic parameters used in the analysis are shown in Table I. Dissociation rates were generally higher than 200000 h^{-1} (14), and the CLtot in control rats was constant at the much higher k_{off} (> 10000 h^{-1}), as shown in Fig. 6. Thus, 20000 h^{-1} was the observed k_{off} in control rats. The CLtot after dosing of UCN-01 at 72.5 nmol/kg to rats given an infusion of hAGP (Pss; 11.9 μM), where the binding of UCN-01 to hAGP could be assumed to be linear, and the *in vitro* measured k_{off} of UCN-01 from hAGP, are given as the observed values. In both groups of rats, the CLtot increased in parallel with k_{off} at low k_{off} values and reached a plateau at higher k_{off} values. The predicted CLtot at the plateau in the control rats was equal to the observed value. Also, in the rats given an infusion of hAGP, the predicted CLtot was close to the observed value. In addition, the effect of k_{off} on the CLtot was found to be different from that in control rats. This implies that the slow dissociation of UCN-01 from hAGP, as well as the high degree of protein binding, further reduces the CLtot.

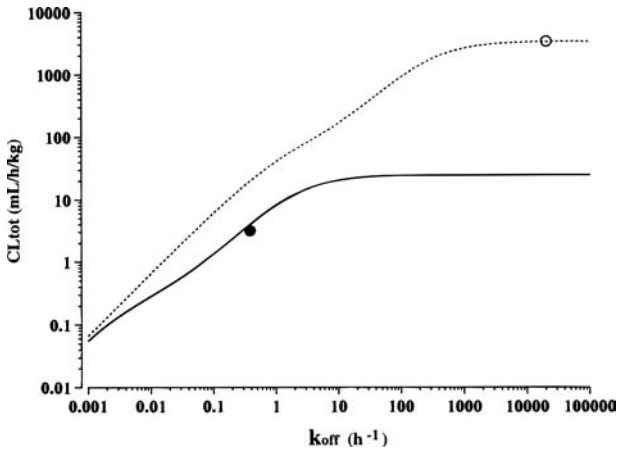

Fig. 6. Relationship between the systemic clearance and dissociation rate constant of UCN-01 in control rats and rats given an infusion of hAGP. The dotted and solid lines represent the simulated data in control rats and rats given an infusion of hAGP. The open and closed circles represent the observed data (*in vitro* k_{off} and *in vivo* CLtot) in control rats and rats given an infusion of hAGP.

Simulation of Plasma Concentration-Time Profiles of UCN-01

The plasma levels of UCN-01 in the rats given an infusion of hAGP were simulated using models incorporating k_{off}/k_{on} or assuming rapid equilibrium of protein binding (Fig. 7). Under the rapid equilibrium conditions generally assumed for protein binding, the simulated plasma concentrations of UCN-01 during the early phase after dosing were approximately one-sixth of the observed values and the elimination was more rapid. On the other hand, the plasma concentration-time profiles simulated

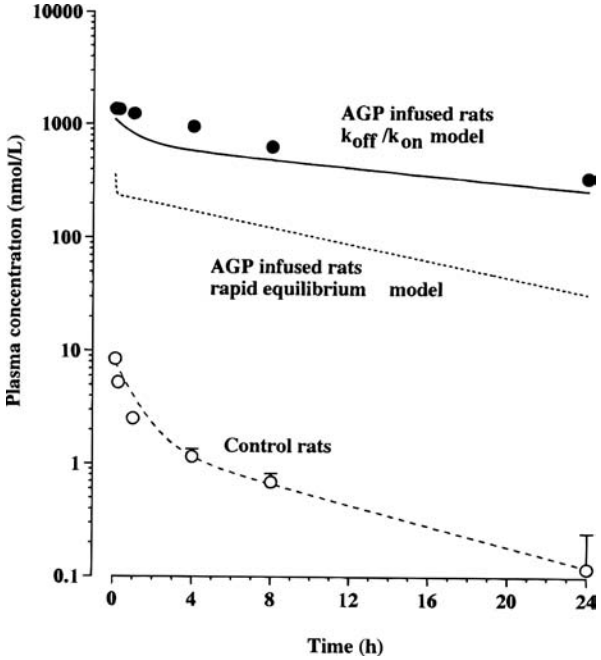

Fig. 7. Comparison of plasma concentration-time profiles simulated by using the models incorporating dissociation/association (solid line) or assuming rapid equilibrium (dotted line) of UCN-01 binding to hAGP. The dashed line represents the simulated data under rapid equilibrium of UCN-01 binding in control rats. The closed and open circles represent the observed data in rats given an infusion of hAGP and control rats.

using the k_{off} (0.383 h^{-1}, Fig. 5) were reasonably close to the observed values.

Simulation of Concentration-Dependence of hAGP and UCN-01

Simulated plasma concentrations of UCN-01 after administering UCN-01 at 725 nmol/kg to rats given an infusion of hAGP (Pss; 0, 1.10 or 11.9 μM) are shown in Fig. 3 and those after administering UCN-01 at 72.5, 725 or 7250 nmol/kg to rats given an infusion of hAGP (Pss; 11.9 μM) are shown in Fig. 4. Although the simulated UCN-01 concentrations exhibited somewhat slower elimination than the observed values at the highest of the tested doses, 7250 nmol/kg, they were comparable with the observed values and the simulation reproduced the altered pharmacokinetics of UCN-01 by hAGP and the non-linear pharmacokinetics of UCN-01.

DISCUSSION

In the phase I studies, UCN-01 exhibited much higher plasma concentrations than predicted from the non-clinical studies in experimental animals and the pharmacokinetics in cancer patients are characterized by an extremely low clearance with a small volume of distribution (1). The marked species-difference in the pharmacokinetics has been suggested to be due to the high degree of binding of UCN-01 to hAGP (1,2). We have previously reported that the simultaneous administration of UCN-01 with equi-molar hAGP to rats increased the plasma concentrations of UCN-01 and reduced the CLtot and Vdss (2). In the previous study, the plasma levels of hAGP after simultaneous bolus administration of UCN-01 gradually declined with a half-life of ca. 17 h and UCN-01 and hAGP were administered only at one dose. In this paper, hAGP levels were maintained at two different levels in rats by constant infusion to mimic the clinical situation and the plasma levels of UCN-01 at three different doses were studied in these animals to clarify the non-linear pharmacokinetics and concentration-dependence of hAGP.

Non-linear pharmacokinetics was exhibited by UCN-01 after bolus iv administration at doses of 72.5, 725 and 7250 nmol/kg to rats with levels of hAGP maintained at about 12 μM (Fig. 4). The UCN-01 concentrations in plasma were saturated around the hAGP levels shown in Fig. 2. Both Vdss and CLtot increased with the dose of UCN-01 and the ratios of Vdss/CLtot were constant at all doses (Table II). This result suggests that the unbound fractions in plasma increased with the dose. On the other hand, the pharmacokinetics of UCN-01 appeared linear in normal rats over the dose range 725 to 7250 nmol/kg (12). Accordingly, the non-linear pharmacokinetics in rats given an infusion of hAGP appears to be due to saturation of the binding of UCN-01 to hAGP.

In a general pharmacokinetic analysis, the association/dissociation of a drug with protein is assumed to reach equilibrium rapidly. The dissociation half-life of UCN-01 from plasma proteins of mice, rats and dogs is presumed to be <0.01 h (2). However, the dissociation half-life of UCN-01 from hAGP was estimated to be approximately 2 h (Fig. 5) and was much longer than that for experimental animals or other drugs, i.e., only a few milliseconds (14). Therefore, a new analysis using a model incorporating the dissociation rate of UCN-01 is required. In order to exclude the effects of other process, e.g., membrane permeability, distribution into tissues, and metabolism, a simple assumption, i.e., the "well-stirred model", was used for these processes. UCN-01 is expected to bind to various proteins such as protein kinases, i.e., targets for UCN-01. Therefore, the attainment of rapid equilibrium in the intracellular space may not happen. However, as described above, this assumption was used since the uptake into isolated rat hepatocytes (2) and the *in vivo* ratio of the UCN-01 concentration in liver to that in plasma (unpublished data) reached constant values relatively rapidly. Further studies may be needed to test the appropriateness of our model, since there is not enough evidence to support this assumption. Assuming the linear condition that UCN-01 concentrations are much lower than nP (hAGP levels), Eq. 5 relating k_{off} to CLtot was introduced from the mass-balance equations in Fig. 1. Eq. 5 is expected to be generally applicable under the condition that the dissociation of ligand from proteins should be considered in the pharmacokinetic analysis. In these circumstances, when each parameter is extrapolated to infinity, the dissociation rate of the ligand from proteins as well as the intrinsic clearance or blood flow rate could limit the distribution/elimination of the ligand. When the association/dissociation of the ligand with proteins was much faster than the blood flow in equation 5, ($Q \cdot R_b$, $Q \cdot R_u << k_{off} \cdot V_E$, $Q \cdot R_b$, $Q \cdot R_u << k_{off} \cdot V_b$, $Q \cdot R_b$, $Q \cdot R_u << k_{on} \cdot nP \cdot V_E$, $Q \cdot R_b$, $Q \cdot R_u << k_{on} \cdot nP \cdot V_b$), the well-stirred model represented by Eq. 9 is obtained from Eq. 5 using Eqs. 7 and 13. Thus, under the condition that the association/dissociation is very rapid, the dissociation rate of the ligand from proteins does not affect the CLtot. Dividing the denominator and nominator of Eq. 5 by $Q \cdot R_b \cdot Q \cdot R_u$ and extrapolating Q to infinity, Eq. 15, below, is obtained.

$$CLtot \rightarrow \frac{CLint \cdot k_{off} \cdot (V_b + V_E)}{\{(k_{on} \cdot nP_u + k_{off}) \cdot (V_E + V_b) + CLint \cdot k_{on} \cdot nP / (k_{on} \cdot nP_u + k_{off})\}} \quad (15)$$

For Eq. 15, when $CLint \cdot k_{on} \cdot nP/(k_{on} \cdot nP_u + k_{off}) \ll (k_{on} \cdot nP_u + k_{off}) \cdot (V_E + V_b)$, CLtot is expressed as $f_p \cdot CLint$, that is, the intrinsic clearance is a limiting factor for CLtot. Subsequently, dividing the denominator and nominator of Eq. 15 by CLint and extrapolating CLint to infinity, the following equation is obtained.

$$CLtot \rightarrow k_{off} \cdot (V_b + V_E)/(1 - f_p) \quad (16)$$

Provided that the dissociation of ligand from protein limits the CLtot completely, CLtot should be the product of k_{off} and the distribution volume for bound ligand ($V_b + V_E$). In the expansion of Eq. 5 from Eqs. 1–4, the assumption that the administered UCN-01 distributes as not only the bound form ($C_{b,a(0)}$) but also as the unbound form ($C_{u,a(0)}$) makes the CLtot in Eq. 16 higher than $k_{off} \cdot (V_b + V_E)$. The relationship between the CLtot and k_{off} in control rats and rats given an infusion of hAGP in the simulation shown in Fig. 6, in a sense, corresponds to a comparison between the ligands or species having different Kd ($= k_{off}/k_{on}$) values. Under the condition ($k_{off} > 7000$ h^{-1}), the constant value of CLtot for rats given an infusion of hAGP was 140-fold lower than that for control rats. The marked reduction is caused by the low Kd, i.e., the high affinity of

UCN-01 for hAGP. In addition, the CLtot at the lowest of the tested doses of UCN-01 is approximately one-eighth that of the constant value of CLtot in Fig. 6. The reduction in the CLtot of UCN-01 can be easily explained by the slow dissociation of UCN-01 from hAGP. This 8-fold difference between the CLtot values at the high k_{off} ($> 7000\ h^{-1}$) and the observed k_{off} ($0.383\ h^{-1}$) reflect the simulation using two models incorporating k_{off} and assuming rapid equilibrium of protein binding in Fig. 7. The simulation using the dissociation-limited model (k_{off}/k_{on}) reproduced the observed plasma concentration-time profiles of UCN-01 adequately, although not well enough since the simulation was conducted using the *in vitro* parameters and not fitting the model to the *in vivo* observed concentrations of UCN-01. On the other hand, the simulated concentrations of UCN-01 under the condition of a rapid equilibrium of protein binding, i.e., very high k_{off}, were lower and eliminated more rapidly than the observed ones. The difference was marked during the initial phase after administration and this result implies that the slow dissociation of UCN-01 from hAGP limits the distribution of UCN-01.

The simulated concentration at 24 h was substantially different from the observed one at a dose of 7250 nmol/kg, i.e., saturated level of binding of UCN-01 to hAGP (Fig. 4). A similar discrepancy between the simulation and the actual situation was found in $t_{1/2}$ at different hAGP levels (Figs. 3, 4). The large individual difference in hAGP at 24 h after dosing of UCN-01 (Fig. 2) may be related to this observation.

The binding of UCN-01 to hAGP can be assumed to be linear since the plasma concentrations of UCN-01, during and after a 3-h infusion at 0.65 and 1.3 mg/m^2 in a Japanese Phase I study ($< 2\ \mu M$, Ref. 1), were much lower than the physiological levels of hAGP (12–71 μM, Ref. 13). In rats given a rapid infusion of hAGP (150 nmol/h/kg), the plasma concentrations of UCN-01 at 72.5 nmol/kg, the lowest of the tested doses, were much lower than the hAGP concentrations (Fig. 2, Fig. 4). Thus, the comparison of the results in rats given an infusion of hAGP with the Japanese Phase I data is meaningful. The Vdss of UCN-01 after administering UCN-01 at 72.5 nmol/kg to rats given an infusion of hAGP, 63.9 ml/kg, was ca. 1/380 that in control rats and was comparable with the Vdss, 79.6–132 ml/kg, in the Phase I study described above (1). On the other hand, the CLtot in the rats given an infusion of hAGP, 3.18 ml/h/kg, fell to ca. 1/1000 that in control rats, 3390 ml/h/kg, but was 40–50 times higher than the value of 0.07 ml/h/kg found in the clinical study. The $t_{1/2}$ in rats given an infusion of hAGP was clearly shorter than that in patients. The discrepancy may be explained by the experimental conditions, such as the shorter period of plasma sampling in this study compared with the Phase I trials. Assuming that several parameters in rats, including the distribution volume for bound and unbound UCN-01 (V_b and V_u) and the intrinsic clearance (CLint), are similar to those in humans, the CLtot in humans was calculated by applying the parameters estimated in humans, namely, the hepatic blood flow and extracellular volume (1243 mL/h/kg and 6.7 mL/kg, Ref. 19), Kd and nP for human plasma (1.25 nM and 16.4 μM, Ref. 1) to Eq. 5. The k_{off} in human plasma, $0.15\ h^{-1}$, was also used. The predicted CLtot in humans was 27 ml/h/kg for the rapid equilibrium model of protein binding (Eq. 9) and 1.1 mL/h/kg for the dissociation-limited model (Eq. 5). Although the latter CLtot was even higher than the observed CLtot in the Phase I studies of UCN-01 (ca. 0.07 mL/h/kg, Ref. 1), the prediction using the dissociation-limited model was more accurate than the former CLtot. In addition, the intrinsic metabolic rate in humans is unknown. A study of the rate of metabolism of UCN-01 is on-going to increase the reliability of the model for clinical studies.

Generally, only unbound drug can cross biological membranes and give rise to pharmacological and toxicological effects. Over the range where UCN-01 concentrations are much lower than hAGP levels in plasma, UCN-01 preferentially exist in the hAGP-bound form. As a result, the CLtot and Vdss of UCN-01 fall and the plasma concentrations increase markedly. In such a situation, the unbound concentrations of UCN-01 in patients should be lower than those in experimental animals having a lower degree of protein binding. However, as shown in the rats given an infusion of hAGP, binding of UCN-01 to hAGP is saturated under the condition that the plasma concentrations of UCN-01 are comparable with the hAGP levels at higher doses of UCN-01. Therefore, it is expected that the unbound concentrations will rise by more than the dose increment and the CLtot and Vdss will also increase. As a result, a small dose increment may lead to toxicity. It is important to measure the unbound concentrations or a marker to predict them in clinical studies. In addition, biologically, several cell types require relatively prolonged exposure in order to be affected by the antiproliferative action of UCN-01, i.e., time-dependent activity (5,22). It would be interesting to see whether unbound UCN-01 exhibits elimination in parallel, i.e., a long half-life, with total UCN-01 or not.

One of the purposes of developing our physiological model is to apply it to clinical studies by using human values such as those obtained for *in vitro* metabolic intrinsic clearance and hepatic blood flow as described above. The model may allow us to evaluate interactions in protein binding and/or metabolism since the effect of individual factors can be isolated using the physiological model, even in cases of combination therapy involving UCN-01 and other anticancer drugs. In order to do this, it is necessary to estimate the Kd and the number of binding sites on hAGP for each drug and the degree of inhibition of the enzymes mediating UCN-01 metabolism by these drugs (e.g., inhibitory constant, Ki) and vice versa. These can be, to some extent, predicted by *in vitro* studies using purified hAGP or human tissues such as liver microsomes and hepatocytes. Although hAGP is known to exhibit inter-patient differences and there are genetic variants (13), the information on the affinity and levels of individual patients or each hAGP variant can be also incorporated into our model. Similarly, it is necessary to estimate approximately the binding parameters in each patient or hAGP-variant. As described above, it is important to predict unbound concentration-time profiles in clinical situations and the prediction of the effects of dose, dosing route, and infusion time on the pharmacokinetic properties of unbound as well as total drug may be expected to reflect the protocols of future clinical studies.

APPENDIX A

Under linear conditions of protein binding, i.e., when plasma concentrations of UCN-01 $<<$ nP_u (P_u = total concentration of hAGP), the equations (Eqs. 1a–4a) are transformed into Laplace forms as shown below:

$$V_E \cdot [s \cdot C_{b,v} - C_{b,v(0)}] = k_{on} \cdot nP_u \cdot V_E \cdot C_{u,v} - k_{off} \cdot C_{b,v} \cdot V_E + Q \cdot R_b \cdot (C_{b,a} - C_{b,v}) \quad \text{(A1)}$$

$$K_{p,u} \cdot V_H \cdot [s \cdot C_{u,v} - C_{u,v(0)}] = k_{off} \cdot C_{b,v} \cdot V_E - k_{on} \cdot nP_u \cdot V_E \cdot C_{u,v} - CLint \cdot C_{u,v} + Q \cdot R_u \cdot (C_{u,a} - C_{u,v}) \quad \text{(A2)}$$

$$V_b \cdot [s \cdot C_{b,a} - C_{b,a(0)}] = k_{on} \cdot nP_u \cdot V_b \cdot C_{u,a} - k_{off} \cdot C_{b,a} \cdot V_b + Q \cdot R_b \cdot (C_{b,v} - C_{b,a}) \quad \text{(A3)}$$

$$V_u \cdot [s \cdot C_{u,a} - C_{u,a(0)}] = k_{off} \cdot C_{b,a} \cdot V_b - k_{on} \cdot nP_u \cdot V_b \cdot C_{u,a} + Q \cdot R_u \cdot (C_{u,v} - C_{u,a}) \quad \text{(A4)}$$

where italic characters represent the Laplace transform as a function of s. On administering UCN-01 into the blood, $C_{b,v(0)}$ and $C_{u,v(0)}$ are both zero (Fig. 1). Applying the infinite theorem, equation (A5) is obtained.

$$\lim_{s \to 0} C_p = AUC_p \quad \text{(A5)}$$

Then, Eqs. (A1–4) can be transformed as follows.

$$0 = k_{on} \cdot nP_u \cdot V_E \cdot AUC_{u,v} - k_{off} \cdot V_E \cdot AUC_{b,v} + Q \cdot Rb \cdot (AUC_{b,a} - AUC_{b,v}) \quad \text{(A6)}$$

$$0 = k_{off} \cdot AUC_{b,v} \cdot V_E - k_{on} \cdot nP_u \cdot V_E \cdot AUC_{u,v} - CLint \cdot AUC_{u,v} \cdot Q \cdot R_u \cdot (AUC_{u,a} - AUC_{u,v}) \quad \text{(A7)}$$

$$V_b \cdot C_{b,a(0)} = k_{off} \cdot AUC_{b,a} \cdot V_b - k_{on} \cdot nP_u \cdot V_b \cdot AUC_{u,a} - Q \cdot R_b \cdot (AUC_{b,v} - AUC_{b,a}) \quad \text{(A8)}$$

$$Vu \cdot C_{u,a(0)} = k_{on} \cdot nP_u \cdot V_b \cdot AUC_{u,a} - k_{off} \cdot V_b \cdot AUC_{b,a} - Q \cdot R_u \cdot (AUC_{u,v} - AUC_{u,a}) \quad \text{(A9)}$$

Sequentially, by using the matrix,

$$\mathbf{A} \cdot \mathbf{X} = \mathbf{B} \quad \text{(A10)}$$

where

$$\mathbf{A} = \begin{bmatrix} Q \cdot R_b & 0 & -(k_{off} \cdot V_E + Q \cdot R_b) & k_{on} \cdot nP_u \cdot V_E \\ 0 & Q \cdot R_u & k_{off} \cdot V_E & -(k_{on} \cdot nP_u \cdot V_E + CLint + Q \cdot R_u) \\ k_{off} \cdot V_b + Q \cdot R_b & -k_{on} \cdot nP_u \cdot V_b & -Q \cdot R_b & 0 \\ -k_{off} \cdot V_b & k_{on} \cdot nP_u \cdot V_b + Q \cdot R_u & 0 & -Q \cdot R_u \end{bmatrix}$$

$$\mathbf{X} = \begin{bmatrix} AUC_{b,a} \\ AUC_{u,a} \\ AUC_{b,v} \\ AUC_{u,v} \end{bmatrix}$$

$$\mathbf{B} = \begin{bmatrix} 0 \\ 0 \\ Vb \cdot C_{b,a(0)} \\ Vu \cdot C_{u,a(0)} \end{bmatrix}$$

$|A|$ represents the determinant of the matrix A and each AUC can be solved as follows.

$$AUC_{b,a} = \frac{\begin{vmatrix} 0 & 0 & -(k_{off} \cdot V_E + Q \cdot R_b) & k_{on} \cdot nP_u \cdot V_E \\ 0 & Q \cdot R_u & k_{off} \cdot V_E & -(k_{on} \cdot nP_u \cdot V_E + CLint + Q \cdot R_u) \\ V_b \cdot C_{b,a(0)} & -k_{on} \cdot nP_u \cdot V_b & -Q \cdot R_b & 0 \\ V_u \cdot C_{u,a(0)} & k_{on} \cdot nP_u \cdot V_b + Q \cdot R_u & 0 & -Q \cdot R_u \end{vmatrix}}{|\mathbf{A}|}$$

$$AUC_{u,a} = \frac{\begin{vmatrix} Q \cdot R_b & 0 & -(k_{off} \cdot V_E + Q \cdot R_b) & k_{on} \cdot nP_u \cdot V_E \\ 0 & 0 & k_{off} \cdot V_E & -(k_{on} \cdot nP_u \cdot V_E + CLint + Q \cdot R_u) \\ k_{off} \cdot V_b + Q \cdot R_b & V_b \cdot C_{b,a(0)} & -Q \cdot R_b & 0 \\ -k_{off} \cdot V_b & V_u \cdot C_{u,a(0)} & 0 & -Q \cdot R_u \end{vmatrix}}{|\mathbf{A}|}$$

$$AUC_{b,v} = \frac{\begin{vmatrix} Q \cdot R_b & 0 & 0 & k_{on} \cdot nP_u \cdot V_E \\ 0 & Q \cdot R_u & 0 & -(k_{on} \cdot nP_u \cdot V_E + CLint + Q \cdot R_u) \\ k_{off} \cdot V_b + Q \cdot R_b & -k_{on} \cdot nP_u \cdot V_b & V_b \cdot C_{b,a,(0)} & 0 \\ -k_{off} \cdot V_b & k_{on} \cdot nP_u \cdot V_b + Q \cdot R_u & V_u \cdot C_{u,a(0)} & -Q \cdot R_u \end{vmatrix}}{|\mathbf{A}|}$$

$$AUC_{u,v} = \frac{\begin{vmatrix} Q \cdot R_b & 0 & -(k_{off} \cdot V_E + Q \cdot R_b) & 0 \\ 0 & Q \cdot R_u & k_{off} \cdot V_E & 0 \\ k_{off} \cdot V_b + Q \cdot R_b & -k_{on} \cdot nP_u \cdot V_b & -Q \cdot R_b & V_b \cdot C_{b,a(0)} \\ -k_{off} \cdot V_b & k_{on} \cdot nP_u \cdot V_b + Q \cdot R_u & 0 & V_u \cdot C_{u,a(0)} \end{vmatrix}}{|\mathbf{A}|}$$

By expanding $AUC_{b,a}$ by the cofactor in the first row,

$$AUC_{b,a} = \frac{V_b \cdot C_{b,a(0)} \cdot \begin{vmatrix} 0 & -(k_{off} \cdot V_E + Q \cdot R_b) & k_{on} \cdot nP_u \cdot V_E \\ Q \cdot R_u & k_{off} \cdot V_E & -(k_{on} \cdot nP_u \cdot V_E + CLint + Q \cdot R_u) \\ k_{on} \cdot nP_u \cdot V_b + Q \cdot R_u & 0 & -Q \cdot R_u \end{vmatrix}}{|\mathbf{A}|} - \frac{V_u \cdot C_{u,a(0)} \cdot \begin{vmatrix} 0 & -(k_{off} \cdot V_E + Q \cdot R_b) & k_{on} \cdot nP_u \cdot V_E \\ Q \cdot R_u & k_{off} \cdot V_E & -(k_{on} \cdot nP_u \cdot V_E + CLint + Q \cdot R_u) \\ -k_{on} \cdot nP_u \cdot V_b & -Q \cdot R_b & 0 \end{vmatrix}}{|\mathbf{A}|}$$

the numerator of the term, $V_b \cdot C_{b,a(0)}$, is as follows:

$$\begin{aligned} &= V_b \cdot C_{b,a(0)} \cdot (k_{off} \cdot V_E \cdot CLint \cdot k_{on} \cdot nP_u \cdot V_b \\ &+ k_{off} \cdot V_E \cdot CLint \cdot Q \cdot R_u + k_{off} \cdot V_E \cdot Q \cdot R_u \cdot k_{on} \cdot nP_u \cdot V_b \\ &+ Q \cdot R_b \cdot k_{on} \cdot nP_u \cdot V_E \cdot k_{on} \cdot nP_u \cdot V_b \\ &+ Q \cdot R_b \cdot k_{on} \cdot nP_u \cdot V_E \cdot Q \cdot R_u + Q \cdot R_b \cdot CLint \cdot k_{on} \cdot nP_u \cdot V_b \\ &+ Q \cdot R_b \cdot CLint \cdot Q \cdot R_u + Q \cdot R_b \cdot Q \cdot R_u \cdot k_{on} \cdot nP_u \cdot V_b) \end{aligned} \quad \text{(A11)}$$

the numerator of the term, $V_u \cdot C_{u,a(0)}$, is as follows.

$$\begin{aligned} &= V_u \cdot C_{u,a(0)} \cdot (k_{off} \cdot V_E \cdot CLint \cdot k_{on} \cdot nP_u \cdot V_b \\ &+ k_{off} \cdot V_E \cdot Q \cdot R_u \cdot k_{on} \cdot nP_u \cdot V_b \\ &+ Q \cdot R_b \cdot k_{on} \cdot nP_u \cdot V_E \cdot k_{on} \cdot nP_u \cdot V_b \\ &+ Q \cdot R_b \cdot CLint \cdot k_{on} \cdot nP_u \cdot V_b \\ &+ Q \cdot R_b \cdot Q \cdot R_u \cdot k_{on} \cdot nP_u \cdot V_b \\ &+ Q \cdot R_u \cdot Q \cdot R_b \cdot k_{on} \cdot nP_u \cdot V_E) \end{aligned} \quad \text{(A12)}$$

By expanding $|A|$ in the first row,

$$A = Q \cdot R_b \cdot \begin{vmatrix} Q \cdot R_u & k_{off} \cdot V_E & -(k_{on} \cdot nP_u \cdot V_E + CLint + Q \cdot R_u) \\ -k_{on} \cdot nP_u \cdot V_b & -Q \cdot R_b & 0 \\ k_{on} \cdot nP_u \cdot V_b + Q \cdot R_u & 0 & -Q \cdot R_u \end{vmatrix}$$

$$+ (k_{off} \cdot V_b + Q \cdot R_b) \cdot \begin{vmatrix} 0 & -(k_{off} \cdot V_E + Q \cdot R_b) & k_{on} \cdot nP_u \cdot V_E \\ Q \cdot R_u & k_{off} \cdot V_E & -(k_{on} \cdot nP_u \cdot V_E + CLint + Q \cdot R_u) \\ k_{on} \cdot nP_u \cdot V_b + Q \cdot R_u & 0 & -Q \cdot R_u \end{vmatrix}$$

$$+ k_{off} \cdot V_b \cdot \begin{vmatrix} 0 & -(k_{off} \cdot V_E + Q \cdot R_b) & k_{on} \cdot nP_u \cdot V_E \\ Q \cdot R_u & k_{off} \cdot V_E & -(k_{on} \cdot nP_u \cdot V_E + CLint + Q \cdot R_u) \\ -k_{on} \cdot nP_u \cdot V_b & -Q \cdot R_b & 0 \end{vmatrix}$$

$$= k_{off} \cdot V_b \cdot k_{off} \cdot V_E \cdot CLint \cdot Q \cdot R_u + k_{off} \cdot V_b \cdot Q \cdot R_b \cdot CLint \cdot Q \cdot R_u$$

$$+ k_{off} \cdot V_E \cdot Q \cdot R_b \cdot CLint \cdot k_{on} \cdot nP_u \cdot V_b + k_{off} \cdot V_E \cdot Q \cdot R_b \cdot CLint \cdot Q \cdot R_u \quad \text{(A13)}$$

therefore, $AUC_{b,a}$ can be represented using (A11), (A12), (A13) as the following equation.

$$AUC_{b,a} = \{(A11) + (A12)\}/(A13)$$

In a similar way, by expanding $AUC_{u,a}$ by the cofactor in the second row, the numerator of the term, $V_b \cdot C_{b,a(0)}$, is as follows:

$$= V_b \cdot C_{b,a(0)} \cdot \{Q \cdot R_b \cdot Q \cdot R_u \cdot k_{off} \cdot V_E + k_{off} \cdot V_E \cdot Q \cdot R_u \cdot k_{off} \cdot V_b$$
$$+ k_{off} \cdot V_E \cdot CLint \cdot k_{off} \cdot V_b + Q \cdot R_b \cdot Q \cdot R_u \cdot k_{off} \cdot V_b$$
$$+ Q \cdot R_b \cdot k_{on} \cdot nP_u \cdot V_E \cdot k_{off} \cdot V_b + Q \cdot R_b \cdot CLint \cdot k_{off} \cdot V_b\} \quad \text{(A14)}$$

the numerator of the term, $V_b \cdot C_{u,a(0)}$, is as follows:

$$= V_u \cdot C_{u,a(0)} \cdot \{k_{off} \cdot V_E \cdot CLint \cdot k_{off} \cdot V_b + k_{off} \cdot V_E \cdot CLint \cdot Q \cdot R_b$$
$$+ k_{off} \cdot V_E \cdot Q \cdot R_u \cdot k_{off} \cdot V_b + k_{off} \cdot V_E \cdot Q \cdot R_u \cdot Q \cdot R_b$$
$$+ Q \cdot R_b \cdot k_{on} \cdot nP_u \cdot V_E \cdot k_{off} \cdot V_b + Q \cdot R_b \cdot CLint \cdot k_{off} \cdot V_b$$
$$+ Q \cdot R_b \cdot Q \cdot R_u \cdot k_{off} \cdot V_b\} \quad \text{(A15)}$$

therefore, $AUC_{u,a}$ is represented using (A13), (A14), (A15) as the following equation.

$$AUC_{u,a} = \{(A14) + (A15)\}/(A13)$$

The CLtot can be determined as follows:

$$CLtot = D/(AUC_{b,a} + AUC_{u,a})$$

where D is dose of UCN-01 and the sum of $V_b \cdot C_{b,a(0)}$ and $V_u \cdot C_{u,a(0)}$. Then, the numerator of CLtot is as follows:

$$D \times (A13) = (k_{off} \cdot V_b \cdot k_{off} \cdot V_E \cdot CLint \cdot Q \cdot R_u$$
$$+ k_{off} \cdot V_b \cdot Q \cdot R_b \cdot CLint \cdot Q \cdot R_u$$
$$+ k_{off} \cdot V_E \cdot Q \cdot R_b \cdot CLint \cdot k_{on} \cdot nP_u \cdot V_b$$
$$+ k_{off} \cdot V_E \cdot Q \cdot R_b \cdot CLint \cdot Q \cdot R_u) \cdot D \quad \text{(A16)}$$

the denominator of CLtot is obtained as (A17).

$$= D \cdot \{Q \cdot R_b \cdot Q \cdot R_u \cdot (k_{on} \cdot nP_u \cdot V_E + k_{on} \cdot nP_u \cdot V_b$$
$$+ k_{off} \cdot V_E + k_{off} \cdot V_b) + Q \cdot R_u \cdot k_{off} \cdot V_E \cdot (k_{on} \cdot nP_u \cdot V_b + k_{off} \cdot V_b)$$
$$+ Q \cdot R_b \cdot k_{on} \cdot nP_u \cdot V_E \cdot (k_{on} \cdot nP_u \cdot V_b + k_{off} \cdot V_b)\}$$
$$+ D \cdot CLint \cdot \{k_{off} \cdot V_E \cdot (k_{on} \cdot nP_u \cdot V_b + k_{off} \cdot V_b)$$
$$+ Q \cdot R_b \cdot (k_{on} \cdot nP_u \cdot V_b + k_{off} \cdot V_b)\}$$
$$+ V_b \cdot C_{b,a(0)} \cdot CLint \cdot (k_{off} \cdot V_E \cdot Q \cdot R_u + Q \cdot R_b \cdot Q \cdot R_u)$$
$$+ V_u \cdot C_{u,a(0)} \cdot CLint \cdot (k_{off} \cdot V_E \cdot Q \cdot R_b) \quad \text{(A17)}$$

Defining the following equation as the condition at time 0:

$$V_b \cdot C_{b,a(0)} = D \cdot k_{on} \cdot nP / (k_{on} \cdot nP + k_{off}),$$
$$V_u \cdot C_{u,a(0)} = D \cdot k_{off} / (k_{on} \cdot nP + k_{off})$$

(A17) is written as follows:

$$= D \cdot \{Q \cdot R_b \cdot Q \cdot R_u \cdot (k_{on} \cdot nP_u \cdot V_E + k_{on} \cdot nP_u \cdot V_b$$
$$+ k_{off} \cdot V_E + k_{off} \cdot V_b) + Q \cdot R_u \cdot k_{off} \cdot V_E \cdot (k_{on} \cdot nP_u \cdot V_b$$
$$+ k_{off} \cdot V_b) + Q \cdot R_b \cdot k_{on} \cdot nP_u \cdot V_E \cdot (k_{on} \cdot nP_u \cdot V_b + k_{off} \cdot V_b)\}$$
$$+ D \cdot CLint \cdot \{k_{off} \cdot V_E \cdot (k_{on} \cdot nP_u \cdot V_b + k_{off} \cdot V_b)$$
$$+ Q \cdot R_b \cdot (k_{on} \cdot nP_u \cdot V_b + k_{off} \cdot V_b)\} + D \cdot CLint \cdot (k_{off} \cdot V_E \cdot Q \cdot R_u$$
$$+ Q \cdot R_b \cdot Q \cdot R_u) \cdot k_{on} \cdot nP / (k_{on} \cdot nP_u + k_{off})$$
$$+ D \cdot CLint \cdot (k_{off} \cdot V_E \cdot Q \cdot R_b) \cdot k_{off} / (k_{on} \cdot nP_u + k_{off}) \quad \text{(A18)}$$

CLtot can be obtained as (A16)/(A18), i.e., Eq. 5 in the text.

APPENDIX B

From the Eq. 7, R_b can be written as follows.

$$R_b = (R - R_u \cdot f_p)/(1 - f_p) \quad \text{(B1)}$$

When C_R represents the concentration in red blood cells, the following equation is obtained.

$$C_R = [Ct \cdot R - Ct \cdot (1 - Ht)]/Ht \quad \text{(B2)}$$

Assuming that the unbound drug concentration in red blood cells is in equilibrium with the unbound drug in plasma, the unbound fraction in red blood cells, f_R, can be written as follows:

$$f_R = f_p \cdot Ht/(R - 1 + Ht) \quad \text{(B3)}$$

so that

$$R = [f_p \cdot Ht + f_R \cdot (1 - Ht)]/f_R) \quad \text{(B4)}$$

substituting (B4) into (B1), and assuming R_u to be one as shown above, Eq. 8 in the text is obtained.

$$R_b = [f_R \cdot (1 - f_p) + Ht \cdot (f_p - f_R)]/f_R/(1 - f_p) \quad (8)$$

REFERENCES

1. E. Fuse, H. Tanii, N. Kurata, H. Kobayashi, Y. Shimada, T. Tamura, Y. Sasaki, Y. Tanigawara, R. D. Lush, D. Headlee, W. D. Figg, S. G. Arbuck, A. M. Senderowicz, E. A. Sausville, S. Akinaga, T. Kuwabara, and S. Kobayashi. Unpredicted clinical pharmacology of UCN-01 caused by specific binding to human α_1-acid glycoprotein. *Cancer Res.* **58**:3248–3253 (1998).
2. E. Fuse, H. Tanii, K. Takai, K. Asanome, N. Kurata, H. Kobayashi, T. Kuwabara, S. Kobayashi, and Y. Sugiyama. Altered pharmacokinetics of a novel anticancer drug, UCN-01 caused by specific high affinity binding to α_1-acid glycoprotein in humans. *Cancer Res.* **59**:1054–1060 (1999).
3. I. Takahashi, E. Kobayashi, K. Asano, M. Yoshida, and H. Nakano. UCN-01, a selective inhibitor of protein kinase C from Streptomyces. *J. Antibiot.* **40**:1782–1784 (1987).

4. S. Akinaga, K. Gomi, M. Morimoto, T. Tamaoki, and M. Okabe. Antitumor activity of UCN-01, a selective inhibitor of protein kinase C, in murine and human tumor models. *Cancer Res.* **51**:4888–4892 (1991).
5. C. M. Seynaeve, M. Stetler-Stevenson, S. Sebers, G. Kaur, E. A. Sausville, and P. J. Worland. Cell cycle arrest and inhibition by the protein kinase antagonist UCN-01 in human breast carcinoma cells. *Cancer Res.* **53**:2081–2086 (1993).
6. S. Akinaga, K. Nomura, K. Gomi, and M. Okabe. Effect of UCN-01, a selective inhibitor of protein kinase C, on the cell-cycle distribution of human epidermoid carcinoma, A431 cells. *Cancer Chemother. Pharmacol.* **33**:273–280 (1994).
7. K. Kawakami, H. Futami, J. Takahara, and K. Yamaguchi. UCN-01, 7-hydroxyl-staurosporine, inhibits kinase activity of cyclin-dependent kinases and reduces the phosphorylation of the retinoblastoma susceptibility gene product in A549 human lung cancer cell line. *Biochem. Biophys. Res. Commun.* **219**:778–783 (1996).
8. T. Akiyama, T. Yoshida, T. Tsujita, M. Shimizu, T. Mizukami, M. Okabe, and S. Akinaga. G1 phase accumulation induced by UCN-01 is associated with dephosphorylation of Rb and CDK2 proteins as well as induction of CDK inhibitor p21/Cip/WAF1/Sdi1 in p53-mutated human epidermoid carcinoma A431 cells. *Cancer Res.* **57**:1495–1501 (1997).
9. S. Akinaga, K. Nomura, K. Gomi, and M. Okabe. Enhancement of antitumor activity of mitomycin C in vitro and in vivo by UCN-01, a selective inhibitor of protein kinase C. *Cancer Chemother. Pharmacol.* **32**:183–189 (1993).
10. S. Akinaga, K. Nomura, K. Gomi, and M. Okabe. Synergistic antitumor effect of UCN-01, a protein kinase (C) inhibitor, combined with various anti-cancer agents. *Proc. Am. Assoc. Cancer Res.* **33**:3072 (1992).
11. R. T. Bunch, and A. Eastman. Enhancement of cisplatin-induced cytotoxicity by 7-hydroxystaurosporine (UCN-01), a new G2-checkpoint inhibitor. *Clin. Cancer Res.* **2**:791–797 (1996).
12. N. Kurata, T. Kuwabara, H. Tanii, E. Fuse, T. Akiyama, S. Akinaga, H. Kobayashi, K. Yamaguchi, and S. Kobayashi. Pharmacokinetics and pharmacodynamics of a novel protein kinase inhibitor, UCN-01. *Cancer Chemother. Pharmacol.* **44**:12–18 (1999).
13. J. M. H. Kremer, J. Wilting, and L. H. M. Janssen. Drug binding to human alpha-1-acid glycoprotein in health and disease. *Pharmacol. Rev.* **40**:1–47 (1988).
14. G. R. Wilkinson. Plasma and tissue binding considerations in drug disposition. *Drug Metab. Rev.* **14**:427–465 (1983).
15. N. Kurata, T. Kuramitsu, H. Tanii, E. Fuse, T. Kuwabara, H. Kobayashi, and S. Kobayashi. Development of a highly sensitive high-performance liquid chromatographic method for measuring an anticancer drug, UCN-01 in human plasma or urine. *J. Chromatogr. B* **708**:223–227 (1998).
16. M. Gibaldi and D. Perrier. Noncompartment analysis based on statistical moment theory. In M. Gibaldi, and D. Perrier (eds.), *Pharmacokinetics*, Marcel Dekker, New York, 1982, pp. 409–417.
17. N. Watari, and L. Z. Benet. Determinant of mean input time, mean residence time, and steady-state volume of distribution with multiple drug inputs. *J. Pharmacokin. Biopharm.* **17**:593–599 (1989).
18. K. S. Pang, and M. Rawland. Hepatic clearance of drugs. I. Theoretical considerations of "well-stirred" model and a "parallel tube" model. Influence of hepatic blood flow, plasma and blood cell binding, and the hepatocellular enzymatic activity on hepatic drug clearance. *J. Pharmacokin. Biopharm.* **5**:625–653 (1977).
19. B. Davies, and T. Morris. Physiological parameters in laboratory animals and humans. *Pharm. Res.* **10**:1093–1095 (1993).
20. T. Fujita, and A. Koshiro. Development of the convenient and direct numerical analytical method of the pharmacokinetics of phenytoin by an ordinary and/or the Bayesian weighted least-squares method using the program MULTI2 (BAYES). *J. Pharmacobio-Dyn.* **12**:717–725 (1989).
21. K. Yamaoka, and T. Nakagawa. A nonlinear least squares program based on differential equations, MULTI (RUNGE), for microcomputers. *J. Pharmacobio-Dyn.* **6**:595–606 (1983).
22. E. Fuse, T. Kobayashi, M. Inaba, and Y. Sugiyama. Prediction of the maximal tolerated dose (MTD) and therapeutic effect of anticancer drugs in humans: integration of pharmacokinetics with pharmacodynamics and toxicodynamics. *Cancer Treat. Rev.* **21**:133–157 (1995).